Half-life of ^{228}Pu and α decay of ^{228}Np

K. Nishio[1], H. Ikezoe[1], S. Mitsuoka[1], K. Satou[1], and C.J. Lin[1,2]

1. *Japan Atomic Energy Research Institute, Tokai-mura, Ibaraki 319-1195, Japan*
2. *China Institute of Atomic Energy, Beijing 102413, China*

Abstract

The neutron deficient nucleus ^{228}Pu was produced in the reaction of ^{34}S+^{198}Pt and the half-life was determined to be $1.1^{+2.0}_{-0.5}$ s. The half-life follows the Geiger-Nuttall curve for even-even Pu isotopes, which shows that α decay is the dominant decay mode. In this reaction, α decay of ^{228}Np was observed for the first time. The evaporation residue cross sections of ^{228}Pu($4n$), ^{228}Np($p3n$) and ^{225}U($\alpha 3n$) are reproduced by a statistical model calculation.

1 Introduction

Plutonium-228 was produced and identified for the first time by Andreyev *et al.*[1] in the fusion reaction of ^{24}Mg+^{208}Pb. However, they were not able to determine the half-life of ^{228}Pu. We produced ^{228}Pu in the fusion reaction ^{34}S+^{198}Pt[2] (compound nucleus ^{232}Pu) and the half-life was determined. For the actinide nuclei with proton number of Z=90−94 and neutron number of N=134−138, α-particle emission and electron capture (EC) are two competing decay modes, suggesting the dominant α-decay mode. For ^{228}Pu, a calculation suggests that the α-decay partial half-life, $T_{\alpha,1/2}$ =0.42 s [3], is two orders of magnitude shorter than that of EC-decay $T_{\mathrm{EC},1/2}$ =44 s [4].

In addition to ^{228}Pu, we have produced ^{228}Np in the same reaction and the α-decay was observed for the first time. The first production of ^{228}Np was made by Kuznetsov *et al.* [5], who determined the half-life of fission activity as 60 s in the reaction ^{22}Ne+^{209}Bi. The EC-delayed fission properties of ^{228}Np was studied by Kreek *et al.* [6] in detail. So far there is no report on the measurement of the α decay of ^{228}Np.

2 Experiment

The ^{34}S ions were accelerated to E_{beam}=170 and 172 MeV by the JAERI-tandem accelerator and irradiated a ^{198}Pt target. The target with thickness 390μg/cm^2 was made by sputtering an enriched ^{198}Pt material (98%) on a 1.2μm thick aluminum (Al) foil. The above bombarding energy corresponds to the center-of-mass energy ($E_{\mathrm{c.m.}}$) of 141 and 143 MeV, respectively, at the half-depth of the target layer.

The evaporation residues emitted in the beam direction were separated in flight from the primary beams by the JAERI-RMS [7]. The JAERI-RMS was set to transport fusion products with 16^+ charge state, which has the the probability of 0.18 in the charge state distribution. The total transport efficiency [8] for $4n$, $p3n$ and $\alpha 3n$ channels are determined

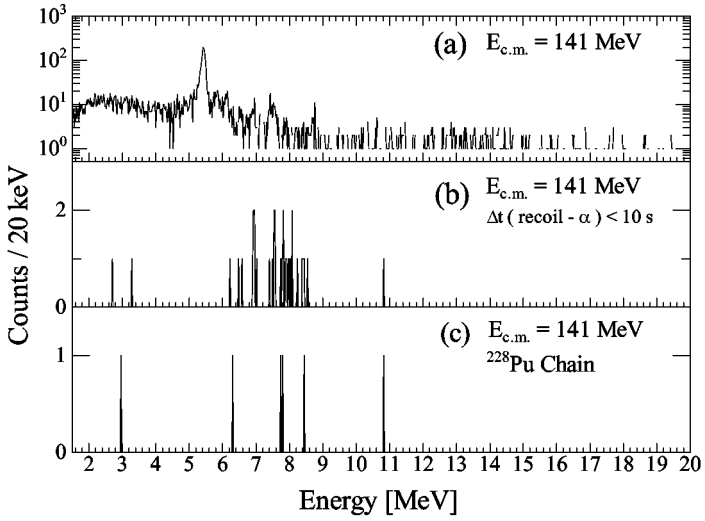

Figure 1: Energy spectra obtained from the PSD in the reaction of ^{34}S+^{198}Pt at $E_{\mathrm{c.m.}}$ =141 MeV.

to be 0.086, 0.074, and 0.050, respectively. The ERs transported through the JAERI-RMS were implanted into a double-sided position-sensitive silicon detector (PSD; 73 × 55 mm^2) located in the focal plane. The identification of the nucleus is made by constructing an α-decay chain and finding the known α-particle energies (and also life-times) of descendants, whose decay position agrees with that of the recoil implantation. The position resolution were 0.15 mm and 0.26 mm in FWHM for X and Y, respectively. Typical energy resolution of the PSD was 75 keV (FWHM).

The α decay in the PSD is distinguished from the transported particle by determining that no time-of-flight (TOF) signal is present, and TOF is measured by two timing detectors separated by the distance of 30 cm and placed upstream the PSD. In the off-line data analysis, the ERs were separated from the scattered beam particles on the two dimensional spectrum of the TOF versus energy. This process considerably reduces the chance coincidence in finding a *recoil*-α correlation. Here, *recoil* means the event of the ER to hit the PSD.

3 Results and Discussions

Figure 1 shows the energy spectrum obtained from the PSD. The spectrum (a) shows the events which do not generate TOF signals and includes all events taken during a 41-hour run at the reaction energy of $E_{\mathrm{c.m.}}$ =141 MeV. The large peak at 5.4 MeV is α-particles from the external α source (^{241}Am) which irradiated the silicon detector during the measurement. The broad 2−6 MeV spectrum is formed by scattered beam particles transported through the JAERI-RMS. As the detection efficiency of the timing detectors was not 100 %, such background particles are not fully rejected and appear in the spectrum (a). There are several α lines in Fig.1 (a) including α decays of ^{216}Th(7921keV,28ms), ^{215}Ac(7604,0.17s), ^{215}Th(7524:7395,1.2s), ^{212}Ra(6899,13s), ^{211}Ra(6.910,13s), ^{211}Fr(6534,3.1min), ^{207}Rn(6131, 9.3min) and ^{207}At(5758,1.8hr). These nuclei are produced, for the calibration purpose, by the reaction of the beam with ^{186}W nucleus contained in the ^{198}Pt target.

The correlation between the recoil implantation and the subsequent α-decays were searched for within the time interval Δt(*recoil*-α) of 10 s. We only selected chains in which the recoil implantation is followed by two or more α-decays. We obtained 18 chains and the corresponding α-particle energy spectrum is shown Fig.1(b). In this process, the condition was imposed that the *recoil* event generates the TOF and energy signal corresponding to the ERs on the two dimensional spectrum to reject chance events associated with the scattered particle.

Among the chains in Fig.1(b), we searched for one that is followed by a long-lived nuclues with the help of position agreement. The searching time is 120 min, long enough to observe the α decay of ^{212}Rn ($T_{1/2}$=23.9min [9]) as the descendant of ^{228}Pu. In this process, we found two decay chains, and the E_α-spectrum is shown in Fig.1(c). They are both attributed to the ^{228}Pu-chain based on their decay character as shown in Table.1. The half-life of ^{228}Pu was determined to be $1.1^{+2.0}_{-0.5}$ s. The obtained average α-particle energy of ^{228}Pu, 7772$\pm$35 keV, reasonably agrees with the data [1]. The present E_α and half-life are compared with the prediction of the Geiger-Nuttall law. In order to determine the α-decay Q-value, Q_α, for ^{228}Pu, we assumed that the detected α decay is from ground-state to ground-state transition, and the electron screening effect [10] is corrected for. The Q_α(7948$\pm$36 keV) and $T_{1/2}$ are plotted in Fig.2 together with the other data [9]. In this figure, the Geiger-Nuttall curves for elements Th, U, and Pu are drawn by using the expression and constants in [10]. Our data of ^{228}Pu follows the characteristics of Pu isotopes. This means that the ^{228}Pu decay is dominated by the α decay.

In order to find the α-decay of ^{228}Np with half-life of 61.4 s [6], the *recoil*-α chain was searched for in the time span of 10 s $\leq \Delta$t(*recoil*-α) $<$ 300 s. We set the condition that the recoil implantation is followed by two or more α-decays in this time region. Five chains starting from ^{228}Np are obtained at $E_{\rm c.m.}$ = 143 MeV, and the decay properties are listed in Table. 2. From the mass table of Audi and Wapstra [11], the α-decay Q value Q_α of ^{228}Np is obtained to be 7415 keV. This results in the α-decay energy of 7285 keV for the ground-state to ground-state α-decay of ^{228}Np. This is 100$-$220 keV larger than the experimental data. A possible reason is that the α decay predominantly produces the excited states of ^{224}Pa.

The obtained ER cross sections for ^{228}Pu, ^{228}Np and ^{225}U are shown in Fig. 3. The errors are in the margin of the statistical error. The data were compared to a statistical model calculation. For this purpose, the partial wave cross section for the fusion ^{34}S+^{198}Pt was calculated by using the CCDEF code [12], which was then inputted to the HIVAP code [13] to calculate the surviving probability and the ER cross section of the specific channel. In the CCDEF code, we took into account the couplings to inelastic channels of the projectile and target. For ^{34}S, deformation parameter (excitation energy) of the quadrupole and octupole vibrations are β_2=0.252 (2.13 MeV) [14] and β_3=0.330 (4.62 MeV) [15], respectively. β_3=0.05 (1.68 MeV) [15] was adopted for the octupole vibration of ^{198}Pt. We also took into account the static deformation of ^{198}Pt (β_2=$-$0.060 [16], β_4=$-$0.030 [17]). The calculated fusion cross section ($\sigma_{\rm fus}$) is shown on the upper section of Fig. 3 by the dashed curve. The dotted curve is the result of the one-dimensional barrier penetration model, which gives the barrier height of 141.1 MeV. The ER cross sections calculated by the HIVAP code are shown by the solid curve in each section of the figure. We have to adjust the factor $b_{\rm fac}$, by which the fission barrier height of the liquid-drop part [18] is multiplied to calculate the fission barrier, $B_{\rm f} = b_{\rm fac}B_{\rm LDM} - \delta W$, from 1.03 [19] to 1.00 so as to obtain reasonable agreement with the experimental data. The δW is the ground state shell energy

Table 1: Alpha-decay energy (in keV) and life-time (given in parenthesis) starting from the recoil implantation of ^{228}Pu ($4n$ channel). The literature value of kinetic energy of α particle and half-life (in square brackets) for ^{228}Pu [1] and the other nuclei [9] is shown in the first line. The time with symbol '<' represents the time interval relative to the preceding α decay. The signal with escaped event is indicated by '*esc*'. The signal of pile up, '*pil*', is caused by the α decays of a mother and a short-lived daughter indicated by '⟵'.

No.	^{228}Pu	^{224}U	^{220}Th	^{216}Ra	^{212}Rn
	7810	8466 [0.9ms]	8790 [9.7μs]	9349 [0.18μs]	6264 [23.9min]
II-1	7807 (0.35s)	–	10817_{pil} (<0.77ms)	⟵	6309 (34min)
II-2	7736 (2.76s)	8446 (3.2ms)	–	–	2960_{esc} (11min)

Table 2: Alpha-decay energy (in keV) and life-time starting from the recoil implantation of ^{228}Np ($p3n$ channel). The literature value for ^{228}Np [6] and the other nuclei [9] is shown in the first line. See the captions of Table 1 for the detailed explanation.

No.	^{228}Np	^{224}Pa	^{220}Ac	^{216}Fr	^{212}At
	– [61.4s]	$7488^{70\%}$ [0.79s]	$7855^{26\%}$ (26.4ms)	9005 [0.7μs]	$7679^{82\%}$,$7045^{0.45\%}$ [0.314s]
III-1	7183 (29s)	7529 (1.10s)	14048_{pil} (3.7ms)	⟵	3170_{esc} (0.070s)
III-2	7062 (128s)	7543 (0.20s)	7794 (58ms)	–	7687 (2.4ms)
III-3	7126 (196s)	7495 (0.56s)	13425_{pil} (21ms)	⟵	7012 (0.12s)
III-4	7177 (35s)	7521 (3.03s)	–	–	7658 (0.18s)
III-5	7065 (15s)	–	–	8969 (<3.39s)	–

correction.

The experimental ER cross section $1.7^{+2.2}_{-1.3}$ nb of the $4n$ channel at $E_{\rm c.m.}$ =141 MeV in the fusion reaction ^{34}S+^{198}Pt was close to 4±2 nb of the $4n$ channel of ^{24}Mg+^{208}Pb reaction at $E_{\rm c.m.}$ =118 MeV [1] which forms the same compound nucleus ^{232}Pu. For the ^{24}Mg+^{208}Pb reaction, we also calculated the cross sections of ^{228}Pu with the same procedure. In the CCDEF calculation, we used deformation parameters β_2=0.606 (1.37 MeV) [14] and β_3=0.250 (7.62 MeV) [15] to take into account the couplings to the excited states of ^{24}Mg. For the excitation of ^{208}Pb, parameters β_2=0.054 (4.09 MeV) [14] and β_3=0.110 (2.61 MeV) [15] are adopted. The calculated result is 6 nb at $E_{\rm c.m.}$=118 MeV, reproducing the experimental data in [1]. Since the excitation energy, $E_{\rm ex}$=43 MeV, of ^{34}S+^{198}Pt at $E_{\rm c.m.}$=141 MeV is close to $E_{\rm ex}$ =44 MeV of ^{24}Mg+^{208}Pb at $E_{\rm c.m.}$=118 MeV, the survival probability for both systems are nearly identical. The fusion cross section given by the CCDEF code is $\sigma_{\rm fus}$ = 69 mb of ^{34}S+^{198}Pt, which agrees with $\sigma_{\rm fus}$ = 184 mb of ^{24}Mg+^{208}Pb within factor of $\sim$ 3.

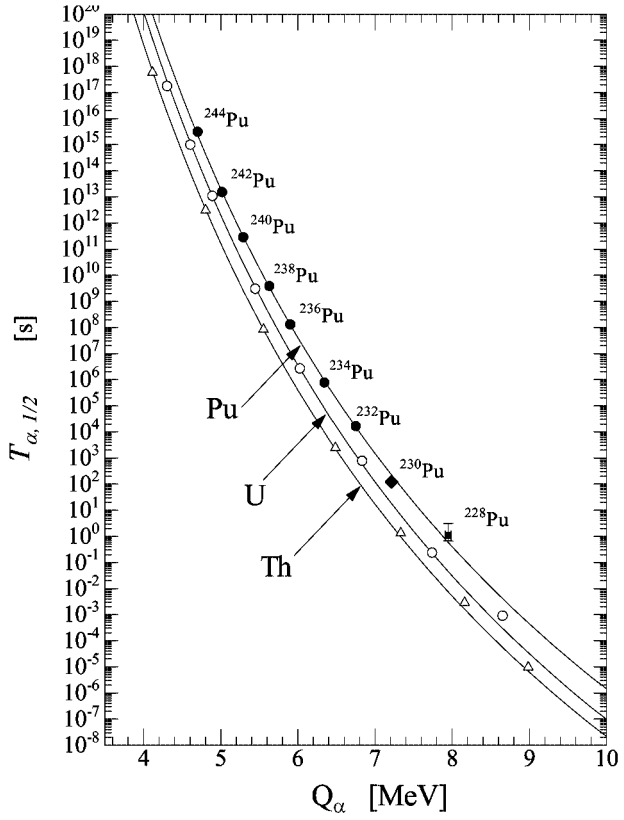

Figure 2: Alpha-decay energy and half-life for ^{228}Pu (solid square with error bar) is plotted on the map of $T_{\alpha,1/2}$ versus Q_α together with the other nuclei (solid circle=Pu, open circle=U, open triangle=Th [9]). The $T_{\alpha,1/2}$-value for ^{230}Pu [20] is shown by the solid diamond. Geiger-Nuttall curve for even-even Pu, U, and Th isotopes [10] are shown by the solid curves.

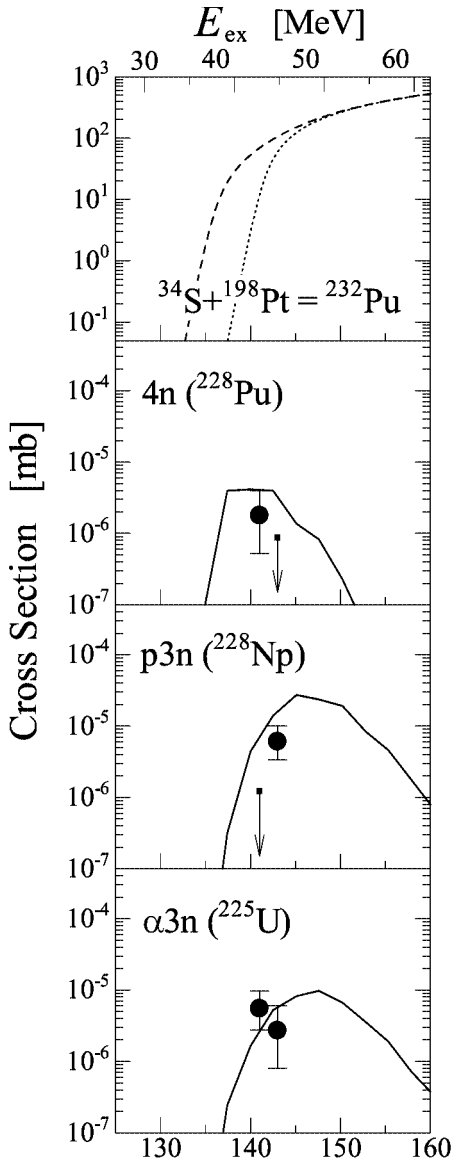

Figure 3: Evaporation residue cross sections for ^{228}Pu, ^{228}Np, and ^{225}U are shown together with the statistical model calculation (solid curve). The vertical bar with arrow shows the upper limit of the cross section. The fusion cross section calculated by the CCDEF code is shown by the dashed-curve, and the fusion cross section of the one-dimensional barrier penetration model is shown by the dotted-curve.

References

[1] A.N. Andreyev *et al.*, Z. Phys. A **347** (1994) 225.

[2] K. Nishio *et al.*, Phys. Rev. C **68** (2003) 064305.

[3] H. Koura, J. Nucl. and Radiochem. Sci., **3**, 201 (2002)

[4] T. Tachibana, M. Yamada, Proc. Inc. Conf. on exotic nuclei and atomic masses, Arles, 1995 (Editions Frontieres, Gif-sur-Yvette, 1995) p.763.

[5] V.I. Kuznetsov, N.K. Skobelev, and G.N. Flerov, Sov. J. Nucl. Phys. **4**, 202 (1967)

[6] S.A. Kreek *et al.*, Phys. Rev. C **50**, 2288 (1994)

[7] H. Ikezoe *et al.*, Nucl. Instrum. Meth. A **376**, 420 (1996)

[8] T. Kuzumaki *et al.*, Nucl. Instrum. Meth. A, **437**, 107 (1999)

[9] R.B. Firestone, Table of Isotopes, edited by V.S. Shirley (Wiley, New York, 1996)

[10] J.O. Rasmussen, 'Alpha, Beta, and Gamma-ray spectroscopy', Vol.1, North-Holland, Amsterdam (1966) pp.701

[11] G. Audi and A.H. Wapstra, Nucl. Phys. **A 595**, 409 (1995)

[12] J.O. Fernández Niello, C.H. Dasso and S. Landowne, Comput. Phys. Commun. **54**, 409 (1989)

[13] W. Reisdorf and M. Schädel, Z. Phys. A **343**, 47 (1992)

[14] S. Raman *et al.*, At. Data and Nucl. Data Tables **36**, 1 (1987)

[15] R. H. Spear, At. Data and Nucl. Data Tables, **42**, 55 (1989)

[16] P. Raghavan, At. Data and Nucl. Data Tables, **42**, 189 (1989)

[17] P. Möller, J.R. Nix, W.D. Myers and W.J. Swiatecki, At. Data and Nucl. Data Tables, **59**, 185 (1995)

[18] S. Cohen, F. Plasil and W.J. Swiatecki, Ann. Phys. **82**, 557 (1974)

[19] K. Nishio *et al.*, Phys. Rev. C, **62**, 014602 (2000), S. Mitsuoka *et al.*, Phys. Rev. C, **62**, 054603 (2000)

[20] P. Cagarda *et al.*, GSI Scientific Report 2001 (2002)